International Journal of Nanomedicine

Dovepress
open access to scientific and medical research

Open Access Full Text Article

ORIGINAL RESEARCH

A Composite Deferoxamine/Black Phosphorus Nanosheet/Gelatin Hydrogel Scaffold for Ischemic Tibial Bone Repair

Dingli Xu[1,2,*], Kaifeng Gan[3,*], Yang Wang[1], Zeting Wu[1], Yulong Wang[1], Song Zhang[1], Yujie Peng[2], Xuguang Fang[4], Hua Wei[5], Yansheng Zhang[5], Weihu Ma[2], Jing Chen[5]

[1]The Affiliated Hospital of Ningbo University Medical School, Ningbo, 315000, People's Republic of China; [2]Ningbo No.6 Hospital, Ningbo, 315000, People's Republic of China; [3]The Affiliated Lihuili Hospital of Ningbo University, Ningbo, 31500, People's Republic of China; [4]The First Affiliated Hospital of Xi 'an Medical University, Xi'an, 710082, People's Republic of China; [5]Zhejiang International Scientific and Technological Cooperative Base of Biomedical Materials and Technology, Zhejiang Engineering Research Center for Biomedical Materials, Cixi Institute of Biomedical Engineering, Ningbo Institute of Materials Technology and Engineering, Chinese Academy of Sciences, Ningbo, 315300, People's Republic of China

*These authors contributed equally to this work

Correspondence: Weihu Ma; Jing Chen, Email 944973034@qq.com; jing.chen@nimte.ac.cn

Introduction: Bone delay union is mostly caused by lack of blood supply. Although autografts, allografts and artificial bone have been widely used to treat bone delay union, the bone regeneration fails in the ischemic site accompanied by the bone donor site complications and disease transmission. Recently, there is a growing recognition of the importance of hydrogel scaffolds which are regarded as an eligible engineer tissue for bone repair. However, hydrogel is still limited in improving neovascularization.

Methods: In this work, black phosphorus nanosheet and deferoxamine (BPN-DFO) were loaded in the gelatin hydrogel to overcome the high risk of bone delay union and systemically investigated the regeneration capability of BPN-DFO hydrogel in vitro and vivo.

Results: The resulting BPN-DFO hydrogel scaffold showed superior swollen, degradation and release rate, as well as satisfied biocompatibility. BPN-DFO hydrogel shown the significant up-expression of mRNA related to bone regeneration and cell proliferation. In vivo, the proposed BPN-DFO hydrogel significantly improved osteogenesis and neovascularization in the ischemic tibial bone site of SD rats with acute femoral artery occlusion. Both macroscopic and histological evaluation of new regenerated bone showed newly formed blood vessel and collagen using BPN-DFO hydrogel. The immunohistochemistry and RT-PCR revealed that the bone regeneration could be improved via BMP/Runx2 pathway.

Conclusion: The BPN-DFO hydrogel possesses potential tissue engineer material for ischemic bone defect treatment. However, furthermore studies are needed to testify the safety and efficacy of BPN-DFO hydrogel.

Keywords: ischemic bone defect regeneration, hydrogel scaffolds, black phosphorus nanosheets, deferoxamine

Introduction

Ischemia plays an important role in bone nonunion.[1] It has been widely recognized that the delayed union or nonunion during bone healing is due to insufficient blood supply.[2] Herbert et al reported that avascular necrosis (AVN) accounted for 13% to 50% of ischemic fracture.[3] Although the bone tissue possesses a good regeneration capability, most of ischemic bone defects cannot fully recover due to insufficient blood supply, which is one of major causes for bone nonunion.[4] When bone nonunion exists, patients may suffer from bone loss, bone deformities and persistent infection, which places a large burden on patients and society (£7000~£50,000 for a single bone fracture nonunion).[5,6]

To date, the widely used clinical strategies for the treatments of bone nonunion have included autogenous bone grafts for small defects, bone transport and induced membrane techniques.[7,8] Although satisfactory clinical recoveries have been reported, a series of unexpected complications have also been observed. Feng et al reported that 15 patients with aseptic recalcitrant humeral shaft nonunion underwent autogenous bone grafting, whose bone union was accompanied by

Received: 3 December 2021
Accepted: 18 February 2022
Published: 11 March 2022

nerve palsy, discomfort and wound infection at the iliac crest.[9] Similarly, Wiss et al reported that 12 of 125 patients with humeral shaft nonunion still failed to heal even after secondary operation.[10]

Recently, hydrogel scaffolds have been recognized as an effective material with various medical values including simple cell or tissue scaffolds, tissue engineering platforms, advanced drug and/or growth factors carrier. Many researchers reported that hydrogel scaffolds achieved clinically desirable regenerative effective in peripheral nerve, spinal cord, wounds, bone and cartilage due to the encapsulation of cells, growth factors and/or bioactive molecules that can be controllably released to improve differentiation and regeneration.[11–13] For a quick and safe bone union, hydrogels are regarded as an optimal scaffold for the regeneration of bone defects due to their good biocompatibility, drug loading and osteoconduction capability. Shah et al prepared the injective hydrogel scaffold based on chondroitin sulphate (CS) and sodium alginate (SA). The cytotoxicity analysis and pharmacokinetic profile of the hydrogel showed that the hydrogel increased the drug release time and had no cytotoxicity toward fibroblasts.[14] Han et al prepared a silver nanoparticles/gelatin hydrogel containing silver nanoparticles (AgNPs) for bone regeneration, which significantly enhanced the alkaline phosphatase (ALP) levels and mineralization in vitro.[15] Similarly, Kamel et al used a calcium-enriched nanofibrillated cellulose hydrogel for bone engineering tissue. In vitro, the biocompatibility and osteogenesis demonstrated a higher level of ALP and calcium ion.[16] It is worth noting that for most of the current studies, osteogenesis in normal bone defects rather than that in ischemic bone defects is the focus of their studies. These scaffolds may induce fibrous tissue formation at the bone defect site under ischemic conditions, resulting in the failure to treat bone defects. Fibrous tissue formation, delayed bone union, nonunion and necrosis will occur due to the lack of bone vascularity during bone defect healing. James et al reported that vascularized graft flap showed superior cartilage quality and survival compared with non-vascularized graft flap for osteochondral grafts in porcine model.[17] Donneys et al reported that activated vascularity at the fracture site can treat delayed unions and nonunion in the mandible of irradiated rat.[18] Therefore, the strategy of bone regeneration with vascularization and osteogenesis may be a superior method when ischemic bone defects exist.[19] To promote bone regeneration at ischemic sites, the scaffolds must be combined with different functions, including osteoconduction, osteogenesis and angiogenesis.

Black phosphorus nanosheet (BPN) and deferoxamine (DFO) become an emerging bioactive component to promote blood vessel and bone regeneration.[20–24] Therefore, we develop a gelatin-methacryloyl (Gelma) hydrogel consisting of BPN and DFO for repairing ischemic bone defect, in which BPN can controllably release phosphorus ion[25] and DFO, as an iron chelator, can promote angiogenesis by activating pivotal proangiogenic genes such as vascular endothelial growth factor (VEGF).[26,27] In vivo animal studies, the femoral artery branches was ligated in all rat. After 3 days, the tibial bone defect in 3mm diameter were created in 40 Wistar rat models. Then, BPN-DFO hydrogel scaffold were implanted into the model rats of the experimental group (N=20), and the tibial bone defects were created in model rats of the control group (N=20) without scaffold implantation.

Experimental Section

Materials

Preparation of BPN-DFO Hydrogel

Briefly, 0.05 g LAP and 1 g GelMA (Engineering for life, China) were fully dissolved in 20 mL PBS at 40 ℃ for 15 min. Subsequently, LAP (Engineering for life, China) (0.25%, w/v) was added into the solution at 60 ℃ for 30 min. 100 μg/mL BPNs (XFNANO, China) and 1 mg/mL DFO (Sigma, American) were then added into the precursor solution. The prepared solution was photo-irradiated using a long-wavelength UV lamp (IntellRay 400, Uvitron, 365 nm, 400 W) for 5 s to prepare the hydrogel scaffold.

Characterization of Hydrogels

The morphological characteristics of BPN-DFO hydrogel scaffolds were observed by SEM (QUANTA 250, FEI, US). To estimate the swelling rate (SR) of the BPN-DFO hydrogel, the swollen test were performed at room temperature over 2 days. First, a dried BPN-DFO hydrogel was weighted (W_0), and then was immersed in 10 mL ultrapure water. The surface water was removed before weighting at each measurement time (W_t). The swelling rate was calculated via the equation: $SR = (W_t - W_0)/W_0 \times 100\%$. The in vitro degradation test in collagenase II PBS solution was conducted at 37

℃ for over 14 days. Every sample was washed with ultrapure water before it was dried for 24 h at each measurement time point (1, 2, 3, 5, 7, 9, 11 and 14 days). Every sample was incubated at 37 ℃ in collagenase II PBS solution. At each measurement, the samples were washed with PBS and were weighed (W_t) after samples were dried at 40 ℃. The degradation rate of BPN-DFO hydrogel was calculated via the equation: $DR = (W_0 - W_t)/W_0 \times 100\%$.

Drug Release Test

In order to study the release rate of phosphorus and ferric ion from the BPN-DFO hydrogels, the drug release assay was performed as follows: For phosphorus ion (P^{5+}), the hydrogel samples were incubated in 1 mL PBS buffer without phosphorus ion at 37℃. 100 μL of supernatant was collected on days 1, 2, 3, 4, 5, 7, 14, 21, followed by the addition of l00 μL fresh buffer.[28] All samples were in triplicate (n = 3). The supernatant samples were analyzed by a phosphorus colorimetric assay kit (Elabscience, China) according to manufacturer's protocol. The release rate of ferric ion (Fe^{2+}) was measured through the similar procedures and was analyzed by ferric colorimetric assay kit (Elabscience, China) at (1, 3, 5, 10, 24, 48, 72, 96 h).

Biocompatibility of BPN-DFO Hydrogel

Live/dead staining was conducted for evaluating the biocompatibility of BPN-DFO hydrogel. Live cells are stained with green fluorescence and dead cells are stained red by calcein-AM and propidium iodide.[29] Precisely, human bone marrow mesenchymal stem cells (BMSCs), which purchased from Mcellbank, Shanghai, China were transferred into a 96-well U-bottom plate and incubated in FBS medium and BNP-DFO hydrogel solution which was prepare by immersing the BNP-DFO hydrogel in DMEM (50 mg/mL) for over 1 and 3 days at 37 °C in the oscillator.[30] Next, the 96-well U-bottom plate was washed with PBS, and was incubated with 2 μmol/L calcein AM and 4 μmol/L propidium iodide for 20 min at room temperature in the dark. Subsequently, the cells were resuspended in PBS. Finally, confocal laser scanning microscope (Zeiss, CLSM 780, Germany) was used to analyze the fluorescence of cells.[31] MTT assay were also performed quantitatively analysis the biocompatibility of BPN-DFO hydrogel.

In vitro Osteogenic Capability

To testify the effect of BPN-DFO hydrogels on the expression of osteogenic differentiation related genes of human bone marrow mesenchymal stem cells (BMSCs). The RT-PCR were carried out to evaluate the mRNA expression of osteogenic related genes. First, the osteogenesis induction medium (OIM) was prepared from phenol red–free α-MEM supplemented with 10% of FBS, 10 mmol/L of β-glycerophosphate, 10 nmol/L dexamethasone, and 50 μg/mL ascorbic acid (All from Sigma, USA).[32] The BMSCs were seeded in a 96-well U-bottom plate and incubated with the BNP-DFO hydrogel or Gelma blank hydrogel in 5% of CO_2 at 37 ℃ in the normal growth medium for 24 h. After that, the medium was replaced with normal growth medium and osteogenesis induction medium. After 7 and 14 days of culture, the total ENA of BMSCs was extracted by TRIzol Reagent (Life Technologies, USA), and the first-strand cDNA of interesting genes were synthesized by Reverse-Transcriptase M-MLV Kits (Takara, Japan). The SYBR Green Kit (Roche, Switzerland) was used to quantify the expressions levels of osteogenesis related genes, and their results were standardized by the expression level of GAPDH (housekeeping gene). The primers sequences of this study were shown in Table S1. The cycling parameters were that 95 °C for 10 min, followed by 40 cycles at 95 °C for 15s, 60 °C for 20s, and 72 °C for 20s.

In vivo Bone Defect Model and Hydrogel Implantation

The animal experiments were approved by the Animal Ethics Committee of Medical School of Ningbo University. All animal surgeries and animal care were performed in a pathogen-free animal experimental room of Ningbo University animal center. After one week of adaptation, ischemic Sprague Dawley (SD) rat model was established by ligating the right femoral artery and branches, and the blood perfusion decreased to 70~80% after 3 days.[33] Totals of 40 male Sprague Dawley (SD) rats were used to establish rat models of bone defects and the hydrogels were implanted under general anesthesia induced by pentobarbital sodium (40 mg/kg). Precisely, the fur of rear leg was removed, then the skin of rear leg sterilized with 75% alcohol. Then the skin was cut along the median of rear leg, and the muscle and periosteum were carefully exposed to create a tibial bone defect 3 mm in diameter with a bone drill (Strong 90 Nanhan, China). The BPN-DFO hydrogel was implanted at the defect site and then irradiated with an ultraviolet lamp (365nm,

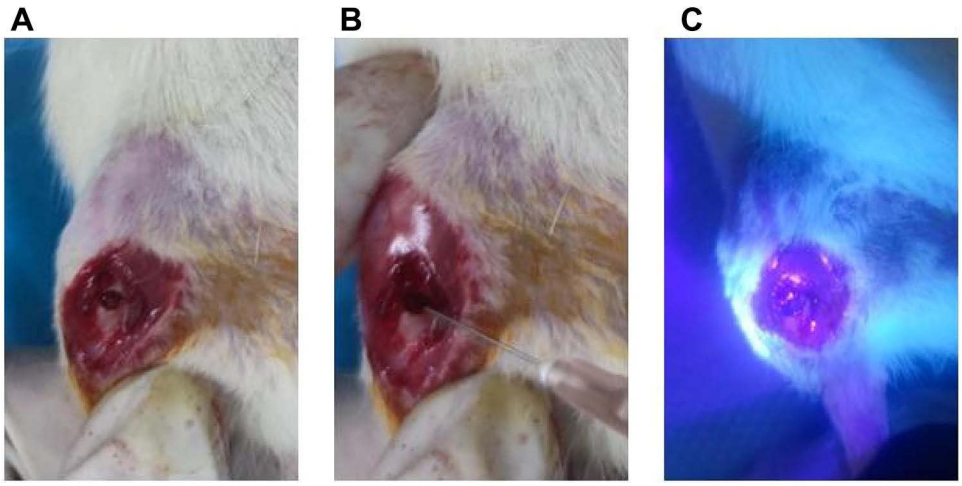

Figure 1 (**A**) cut the skin and created 3mm diameter of tibial bone defects. (**B**) placed the BPN-DFO hydrogel in the defect. (**C**) hydrogels photo-crosslinking using 365 nm ultraviolet lamp irradiation.

UV0003 HY, China) irradiation (Figure 1). After that, the periosteum, muscle and skin were closed layer by layer. For the rats in control group, the hydrogel was implanted after the tibial bone defect was created. After operation, the animals were fed penicillin for 1 week. Ten rats were sacrificed, and then histological evaluation was performed on 5 samples (immunohistochemical analysis was performed on 2 of 5 samples). The RT-PCR test was conducted on the other 5 samples in two groups at weeks 2 and 4 after graft.

Macroscopic and Histological Evaluation

Macroscopic and histological grading scale was used to evaluate the bone repair of each tibia after 2 and 4 weeks. The macroscopic evaluation contains the defect coverage and defect surface and, the histological evaluation contains cell distribution of defect site, bone defect surface, bone matrix (Table 1). The macroscopic and histological evaluation criteria in this study was based on the one reported by Jennifer et al.[34] After macroscopic evaluation, the tibial specimens were fixed in 4% paraformaldehyde and decalcified with 10% EDTA decalcifying solution for 4 weeks. Then all of specimens were then processed for paraffin embedding, and each defect serial sectioned to 5 μm thickness with a rotary microtome and stained with hematoxylin and eosin (H&E). Histological evaluation was performed in the regenerated bones. Masson trichrome stain was used to evaluate bone maturation, because mature bone matrix was stained blue and immature new bone matrix, including muscle fiber and cellulose was stained red.[35]

In immunohistochemical analysis, tibial samples were fixed in 4% paraformaldehyde for 48 h and was decalcified with 10% EDTA decalcifying solution for 4 weeks. The defect with a thickness of 5 μm was sectioned by a rotary microtome after embedding in paraffin. During the rinse step, bone sections were deparaffinized and rehydrated in Tris-buffered saline. Precisely, sections were incubated in 0.3% hydrogen peroxide and Tris-buffered saline before antigen retrieval with citrate buffer (pH 6) at 90 °C. Then air-dried bone sections were permeabilized in 0.3% Triton X-100 for 10 min. The specimen was blocked in 5% goat serum at room temperature for 30 min, and then was incubated with primary antibodies diluted in 5% goat serum in PBS overnight at 4 °C. The primary antibodies were as follows: CD 31 (NB100-2284, Novus, 1:200) and Collagen type 1 (ab34710, Abcam, 1:200). After that, all sections were rinsed three times with PBS and incubated with appropriate Flour-coupled secondary antibodies (Molecular Probes, Life Tech, US, 1:400) for 1 h at room temperature. At last, coverslips were sealed with nail polish and the sections were analyzed under microscopy.

The RNA sequences of tibial bone samples were detected by qRT-PCR for the analysis of the possible molecular mechanism of neo-angiogenesis and osteogenesis of BPN-DFO hydrogel. Precisely, RNA from grinding fluid of tibial tissues was extracted by TRIzol reagent (Invitrogen, Karlsruhe, Germany). Samples with an A260/A280 ratio ranging from 1.8~2.0 was considered eligible, and then was evaluated by DS-11 spectrophotometer machine (DeNovix, Wilmington, DE, USA). Quantitative reverse transcription-polymerase chain reaction (qRT-PCR) analysis was performed

Table 1 The Macroscopic and Histological Evaluation of Regeneration Bone Tissue

Macroscopic Evaluation		**Points**
Defect coverage		
	>75%	4
	50~75%	3
	25~50%	2
	<25%	1
	0%	0
Defect surface		
	Intact bone	3
	Small fissure	2
	Large fissure	1
	Necrosis	0
Integration with bone		
	Complete	3
	>50%	2
	<50%	1
	Demarcation>1mm	0
Histological evaluation		
Cell distribution		
	Uniform	4
	Uniform/clusters	3
	Clusters	2
	Individual cells	1
	Disorganized	0
Surface		
	Continuous smooth	2
	Continuous irregular	1
	Discontinuous	0
Matrix of new bone		
	Mature	2
	Partial mature	1
	Immature	0
Tissue of new bone		
	Normal	3
	Increased remodeling	2
	Necrosis or granulation tissue	1
	Fracture or callus at base	0

by Mx3005P real-time PCR System (Stratagene, La Jolla, CA, USA) and GoTaq qPCR Master Mix (Promega). The sequences of divergent primers of rats were designed and produced as Table S2, and their results were standardized by the expression level of RSP 18.[36]

Statistical Analysis

All the experiments were conducted in triplicate to improve the veracity, and SPSS (SPSS 20.0, Chicago, IL, USA) was used to analyze the data by mean ± SD. In this study, one-way analysis of variance (ANOVA) was used for inter group comparison and the *p*-values less than 0.05 were considered statistically significant.

Results

Characterization of BPN-DFO Hydrogels

The hydrogels were successfully fabricated by aforementioned methods and SEM was used to figure out the micro-morphology of BPN-DFO hydrogel, as shown in Figure S1. The BPN-DFO hydrogel showed a typical porous structure after lyophilization, which is beneficial to cell growth and nutrition supply.[29]

The swelling capacity of hydrogels is evaluated by immersing samples in ultrapure water. As shown in Figure 2A, the BPN-DFO hydrogel displays a higher swelling rate than the blank hydrogel. Besides, the degradation rate can reflect the mass loss in vitro. The analysis of weight loss during incubation is illustrated in Figure 2B. The BPN-DFO hydrogel achieves a higher swelling and degradation rate. This may be due to the increase in the ionic component in the composition of the hydrogels can increase the swelling rate,[37] and the better degradation rate may result from that the nanocomposites and BPN enhancing the hydrophilicity of the hydrogel.[38] More space can be permit osteoblast, vascular endothelial cell and new tissue grow after BPN-DFO hydrogel degraded in time.

The release of phosphorus and ferric ion from the BPN-DFO hydrogel is illustrated in Figure 3. As mentioned above, rapid biomolecule release restricts their efficacy in long-term bone tissue regeneration,[39] and the sustained phosphorus ion release plays a key role in osteogenesis which helps to synergistically improve angiogenesis in bone graft site.[40] From the result, the release cumulative percentage of phosphorus ion showed a sustained release which can constantly improve osteogenesis at the bone defect site. Similarly, a profile of initial burst release of ferric ion in the first 24 h with a constantly slow release after 48 h was observed (Figure 3).

Biocompatibility of BPN-DFO Hydrogel

Human bone marrow mesenchymal stem cells (hBMSC) were cultured in FBS medium with the BNP-DFO hydrogel. The MTT assay and live/dead staining test were subsequently conducted for evaluating the biocompatibility of BNP-DFO hydrogel. The MTT assay are shown in Figure S2, indicating abundant proliferation of hBMSC. As mentioned above, live cells will be stained green by calcein-AM and dead cells stained red by propidium iodide, which means than the more parts that are stained green, the better biocompatibility of this material. The fluorescence images of cells on days 1 and 3 are shown in Figure 4. An adequate proliferation of live cells (Green) was found on days 1 and 3, meaning that the

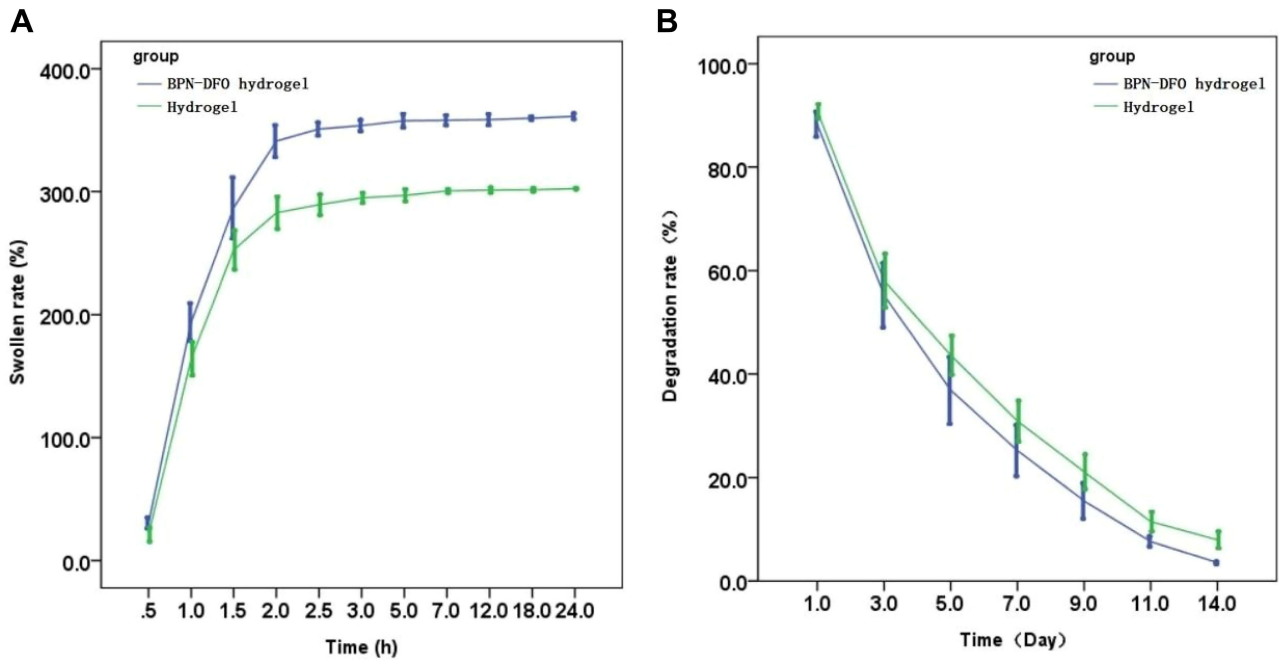

Figure 2 (**A**) Swelling rate of the BPN-DFO hydrogel and hydrogel in ultrapure water at room temperature. (**B**) Degradation rate of the BPN-DFO hydrogel and hydrogel.

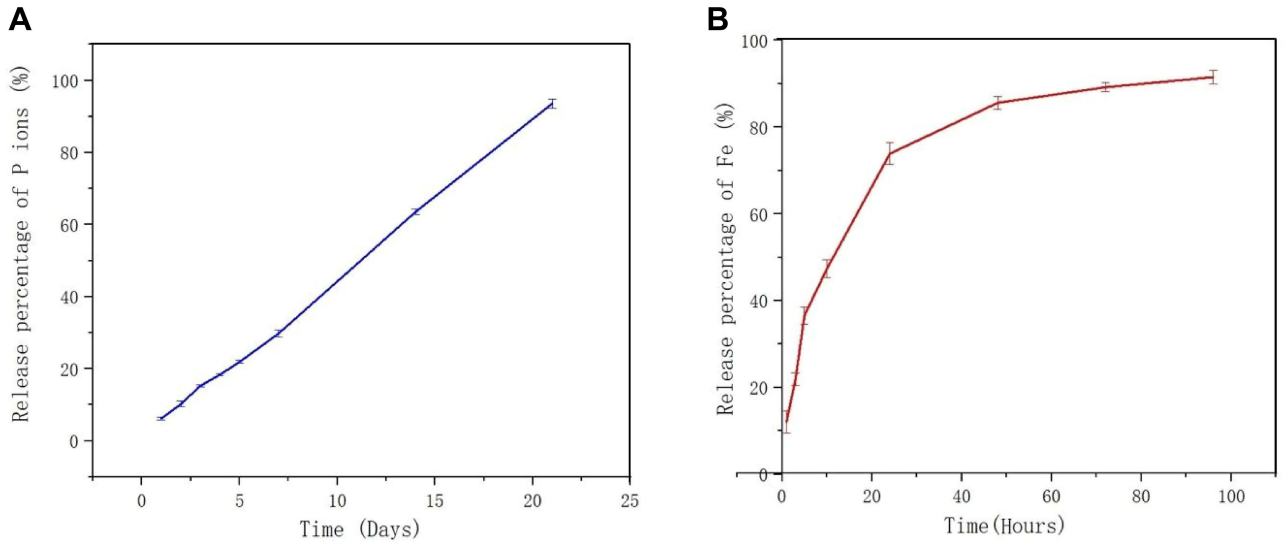

Figure 3 Vitro phosphorus and ferric ion release cumulative percentage of BPN-DFO hydrogel. (**A**) The release cumulative percentage of phosphorus ion showed a sustained release during 21 days. (**B**) The release cumulative percentage of ferric ion are burst during the initial 24 h, then a constantly slow release after 48 h.

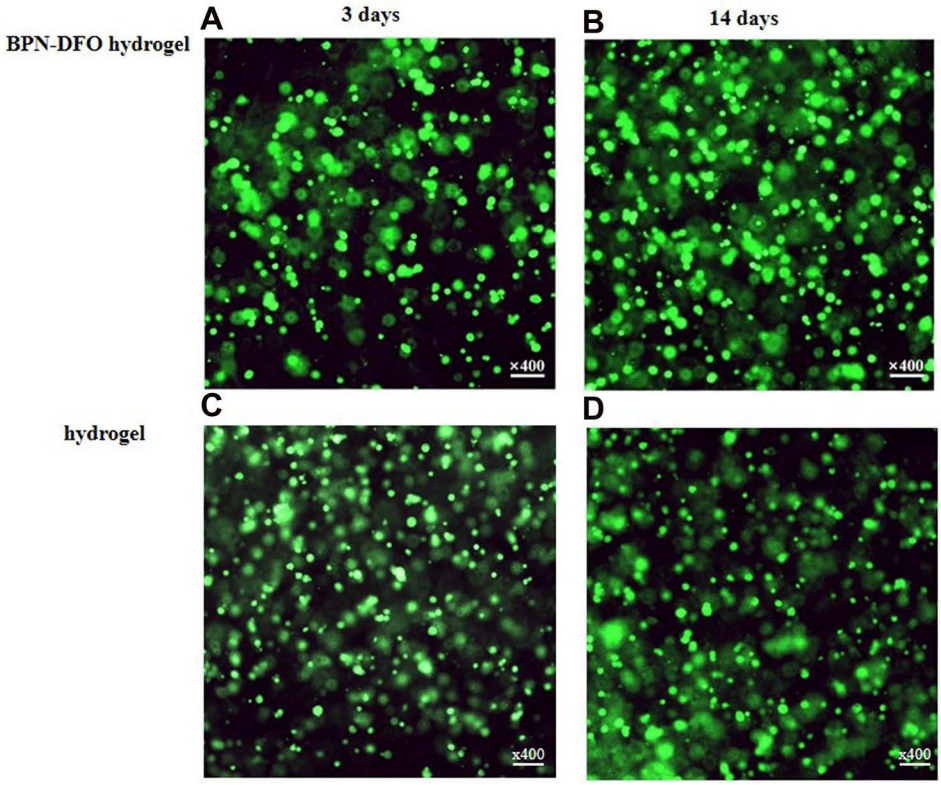

Figure 4 The live/dead stain fluorescence image of hBMSCs incubated at 1 and 3 days in two groups, respectively, and there were no dead cells (red) in two group. (**A**, **B**) The live/dead stain fluorescence image of BPN-DFO group. (**C**, **D**) The live/dead stain fluorescence image of hydrogel group.

BPN-DFO hydrogel has no cytotoxicity impact on hBMSC. Figure 4 illustrates the abundant proliferation and satisfactory cell morphology of hBMSCs on days 1 and 3 that can verify good biocompatibility of BPN-DFO hydrogel. This result indicates that the BPN-DFO hydrogel has great potential to be used as a biocompatible scaffold for bone

regeneration. And Huang et al reported the similar results that black phosphorus hydrogels have satisfactory biocompatibility which verified by live/dead staining.[30]

In vitro Osteogenic Capability of BPN-DFO Hydrogel

RT-PCR tests were conducted to clarify the capability of BPN-DFO hydrogels on the expression of osteogenic differentiation related genes of human bone marrow mesenchymal stem cells (hBMSC) (Figure 5). Osteogenesis is a complex process involving a lot of regulatory factors. In this study, type I pro-collagen (Col-I), bone morphogenetic protein 4 (BMP4), and runt-related transcription factor 2 (RUNX2) were selected because they are widely accepted as important markers for osteogenesis.[41] Col-I, BMP4 and RUNX2 were all up-regulated in the BNP-DFO hydrogel group, with a significantly higher degree than that in hydrogel group after 7 and 14 days of incubation, indicating that the BPN-DFO hydrogel can promote the osteogenesis of hBMSC in vitro effectively and enduringly.

In vivo Bone Defect Model and Hydrogel Implantation

The macroscopic evaluation of the samples was performed and compared at weeks 2 and 4. The full-thickness defects of BPN-DFO group were regenerated with granulation tissue at 2 weeks, whereas there was still a large unfilled defect site in hydrogel group (Figure 6). After 4 weeks of implantation, all defects were repaired with intact bone tissue in BPN-DFO group. However, the defects were repaired with some fissure bone tissue hydrogel group, and the new born bone did not fully integrate with surrounding bone (Figure 6). And there was a significant difference in macroscopic and histological evaluation between two groups at weeks 2 and 4 (6.24±0.68 VS 2.49±0.51; 9.36±0.48 VS 5.82±0.69.

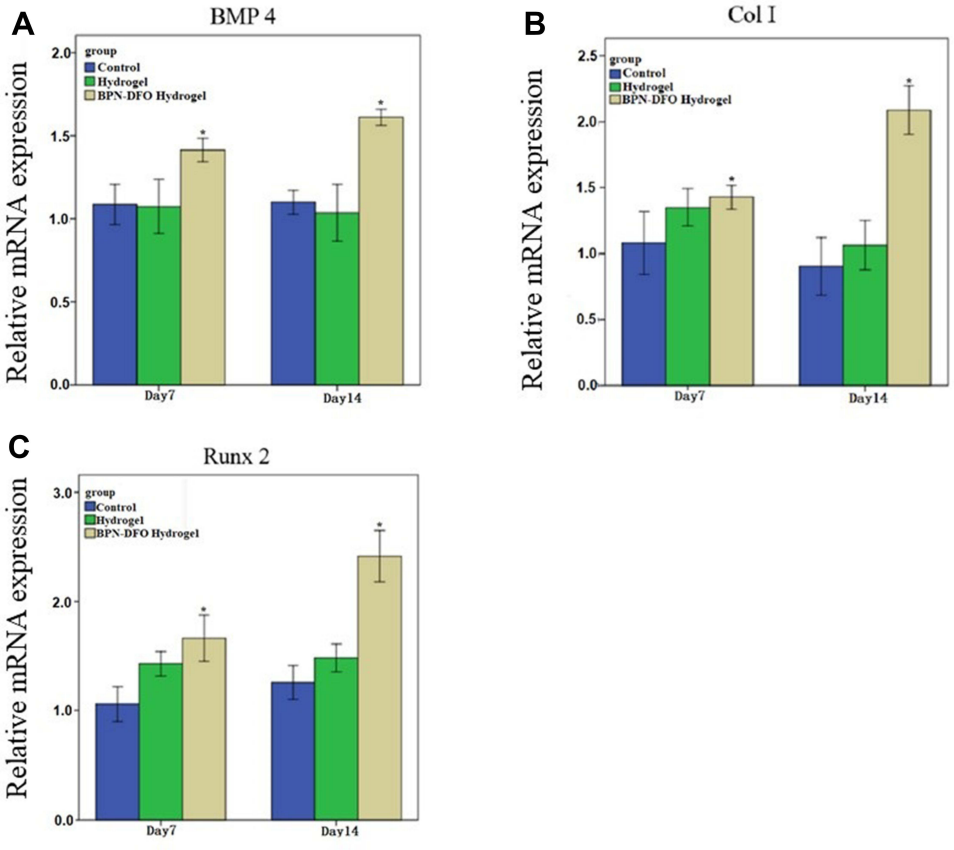

Figure 5 Summarized data showing the effect of BPN-DFO hydrogel and hydrogel on mRNA expression of osteogenic differentiation related genes including Col-I, BMP4 and Runx2 after culturing for 7 and 14 days in vitro. (**A**) The expression of Col I in BPN-DFO group showed significantly improved than control group and hydrogel group at 7 and 14 days. (**B**) The expression of BMP4 in BPN-DFO group showed significantly improved than control group and hydrogel group at 7 and 14 days. (**C**) The expression of Runx 2 in BPN-DFO group showed significantly improved than control group and hydrogel group at 7 and 14 days. (*, $p<0.05$).

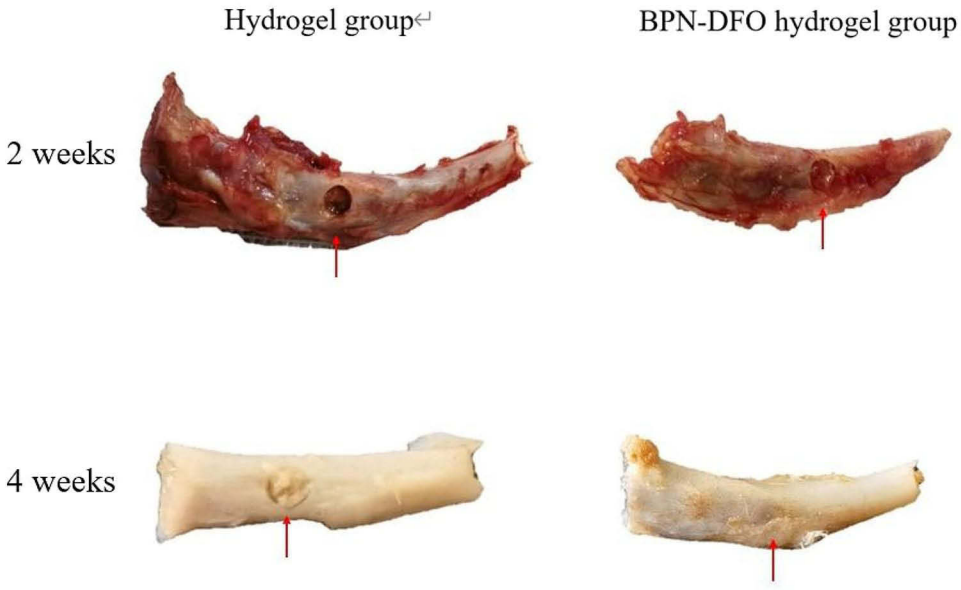

Figure 6 The macroscopic presence of bone defect site in tibial. 2 and 4 weeks in BPN-DFO hydrogel group and hydrogel group.

$P<0.05$) (Table 2). The bone surface completely recovered in BPN-DFO hydrogel group at week 4 (Figure 6), which primarily illustrated that BPN-DFO yielded superior bone regeneration and vascularization in bone defects.[42]

Histology and Immunohistochemistry Analysis

In histological evaluation, the H&E staining was used for the staining of the regeneration tissue of tibial bones to identify its quality. After 2 weeks, H&E staining showed that the new born bone and blood vessel of the BPN-DFO hydrogel group were mainly repaired without undegraded implantation at the bone defect site, with the histological scale at 7.41 ±0.73. However, in the hydrogel group, the bone defects were partially repaired, and there were some undegraded hydrogels at the bone defect site. And the histological scale was 3.52±0.51 ($P<0.05$). Another significant meaningful point was that new blood vessels were ingrowth in BPN-DFO hydrogel group. After 4 weeks of implantation in BPN-DFO hydrogel group, the new bone regeneration fully repaired the bone defect site with mature bone tissue and vascularization. Besides, in the regenerated tissue there were better columnar organization and better integration than that in hydrogel group (Figure 7). Compared with the hydrogel group, more new cells, dense collagen and blood vessels were observed at the bone defect site in BPN-DFO hydrogel group. What's more, new born bone and blood vessel were

Table 2 Comparison of Macroscopic and Histology Scale Between Two Group

Group	Macroscopic	Histology
2 weeks		
BPN-DFO hydrogel	6.24±0.68	7.41±0.73
Hydrogel	2.49±0.51	3.52±0.51
P value	<0.05	<0.05
4 weeks		
BPN-DFO hydrogel	9.36±0.48	10.21±0.69
Hydrogel	5.82±0.69	7.02±0.59
P value	<0.05	<0.05

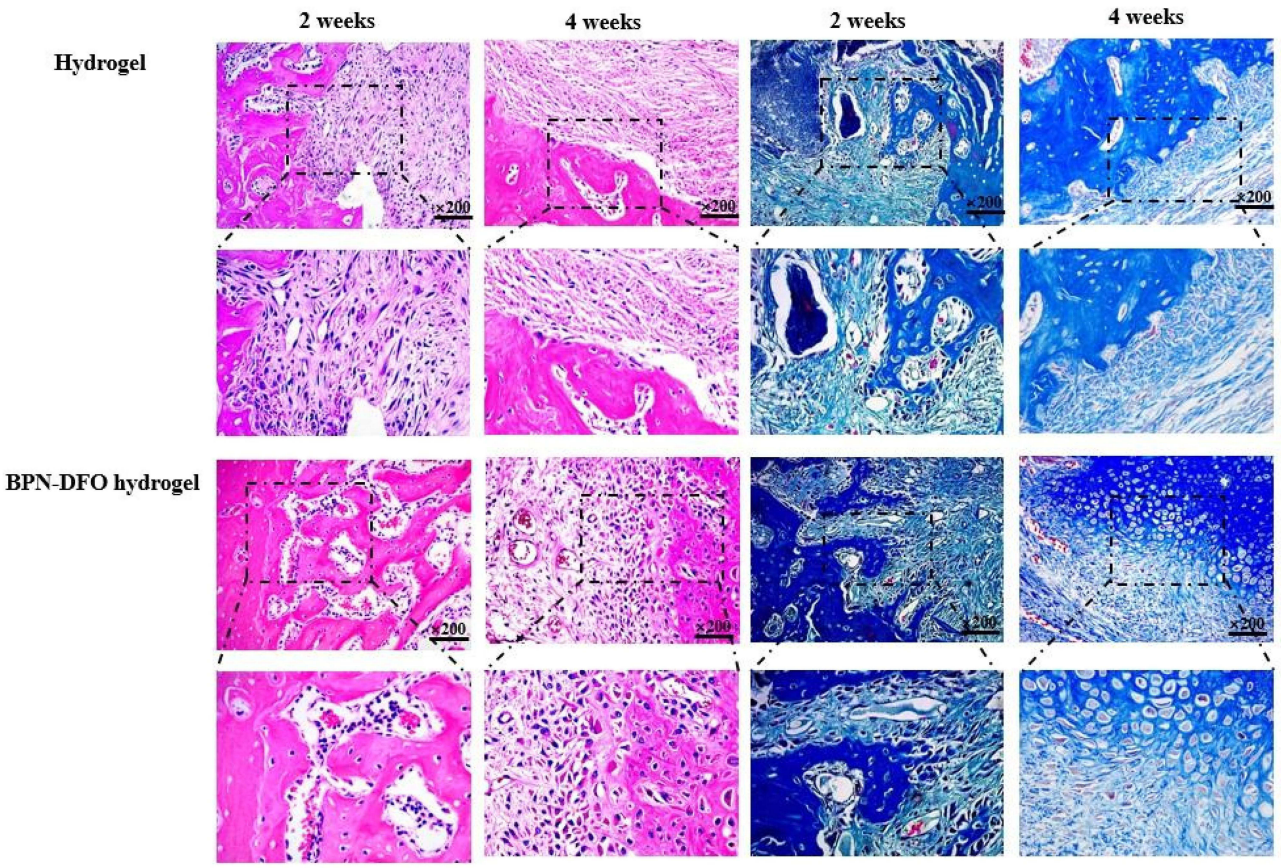

Figure 7 Bone defect repair in the tibial model. H&E staining and Masson staining of histological sections were performed 2 and 4 weeks after implantation. The left part is H&E staining and right part is Masson staining.

formed at the center of bone defect site more than 2 weeks. These results suggested that BPN-DFO hydrogel can have a promote osteogenesis and angiogenesis and inhabit the grow of fibrous tissue.

Masson staining was used to analyze the collagen and new born bone. According to Masson's trichrome staining, mature bone matrix (collagenous tissue) is stained blue, muscle fibrous tissues are stained red (Figure 7), and red blood cells can also be stained red. In BPN-DFO hydrogel group, the newly formed collagens (blue) and blood vessel (red) vessels were obvious. In contrast, only little new immature bone matrix (mainly including muscle fibrous, partially collagens and undegraded hydrogels) can be observed in hydrogel group at week 2 which was similar to the results of H&E staining. Besides, disordered arrangement of cell organization and undegraded implantations (blue) were observed in hydrogel groups, while those phenomena was not observed in BPN-DFO group, indicating that BPN-DFO hydrogel can improve the ability of osteogenesis and angiogenesis. After 4 weeks, little mature bone and newly formed blood vessel were observed at the defect site which was filled with loose and disordered fibrous tissue in hydrogel group, while there were much mature bone matrix and more blood vessels in the BPN-DFO group, and it could be seen that well-arranged collagens were stained deep blue and there were more blood vessels growing at the bone defect site. Such experimental results as the growth of new blood vessels and mature bone matrix indicate that BPN-DFO hydrogel has the ability of osteogenesis and angiogenesis. H&E and Masson staining indicated there was no inflammatory response or necrosis in the newly formed fibrous tissue in all groups. However, dense and mature newly formed fibrous tissue and neovascularization were observed in BPN-DFO group, indicating blood supply can promote the formation of fibrous tissue.[26] On the contrary, there were some loose newly formed fibrous tissue and undegraded hydrogel, but no neovascularization existed in the hydrogel group.

The immunohistochemical analysis was performed on the tissue sections both BPN-DFO hydrogel group and hydrogel (Figure 8). The results showed that much more immunofluorescence (Col I and CD31), which mainly

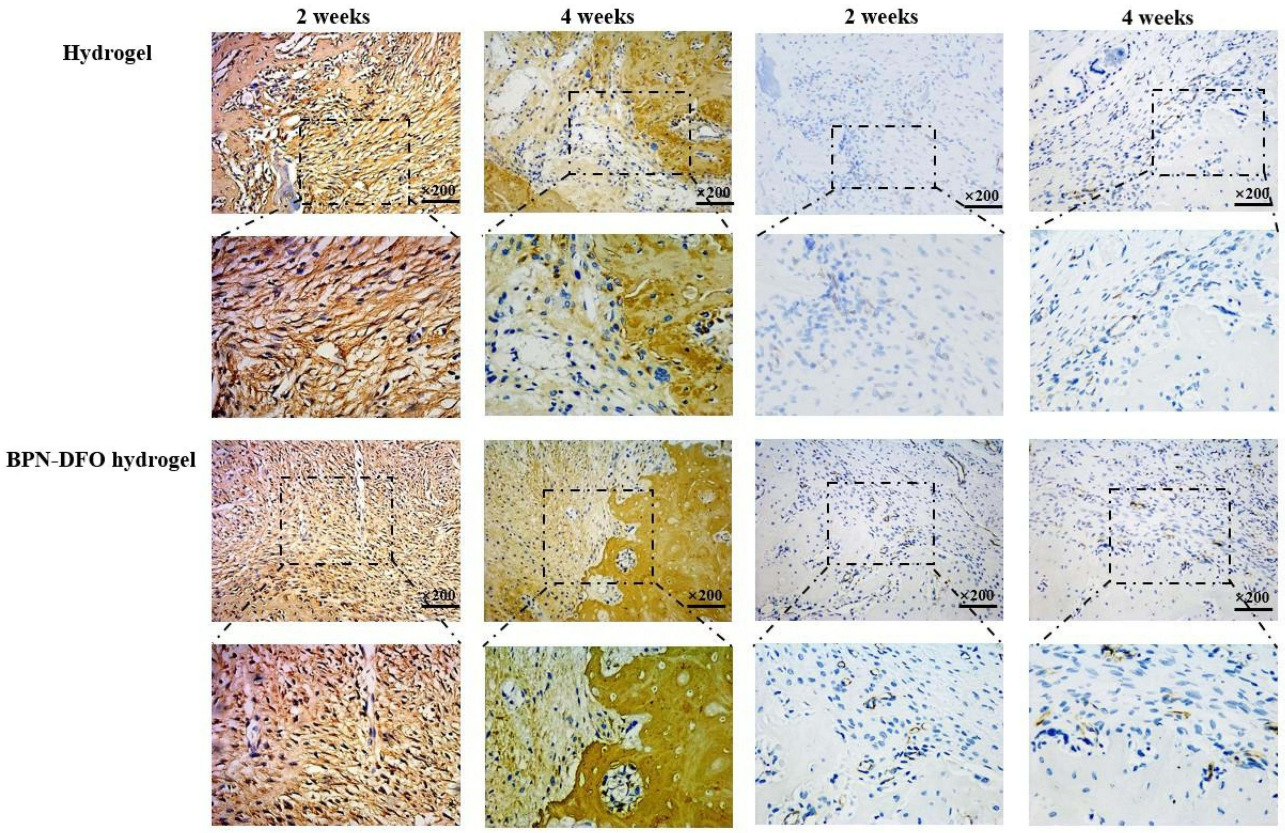

Figure 8 Bone defect repair in the tibial model. Immunohistochemistry analysis (COL I, CD31) of sections were performed 2 and 4 weeks after implantation. The left part is IHC of COL I and right part is IHC of CD 31. And in these two parts, tawny color meaning the positive, which present COL I and CD 31, respectively.

distributed around the osteoblasts in an orderly manner in BPN-DFO group, indicating that the sustained release of phosphorus and ferric iron may upregulate the expression of type I collagens and CD 31 then further activates specific biological activities. What's more, much more blood vessels and mature bone matrix were observed in the BPN-DFO hydrogel group, revealing the relationship between underlying molecular mechanism and the function of angiogenesis and osteogenesis. Furthermore, the images of 4 weeks showed that much more CD 31 and Col I immunofluorescence were observed in the center of bone defect site than that at week 2.

PCR Detection of Tibial Sample Grinding Fluid

The qRT-PCR of the tibial samples showed that BMP4 and Runx2 were significantly upregulated in BPN-DFO hydrogel group on days 14 and 28, respectively (Figure 9), indicating the released phosphorus and ferric ion can improve the osteogenic differentiation. And the obvious upregulation of BPM4 and Runx2 suggested that BPN-DFO hydrogel can benefit osteogenic differentiation.

Discussion

This study analyzed the function of BPN-DFO hydrogel for osteogenesis and angiogenesis in vitro and vivo. And demonstrating the good biocompatibility, controllable drug release and osteogenic capability after BPN-DFO hydrogel fabricated. Then BPN-DFO hydrogel was implanted into rat model of ischemic tibial bone defect in order to verify the ability of angiogenesis and osteogenesis in vivo. The significantly improved defect regeneration by the BPN-DFO hydrogel showed that sustained release of phosphorus and ferric ion and osteoconductive of hydrogels may improve bone regeneration via Bmp/Runx 2 pathway.

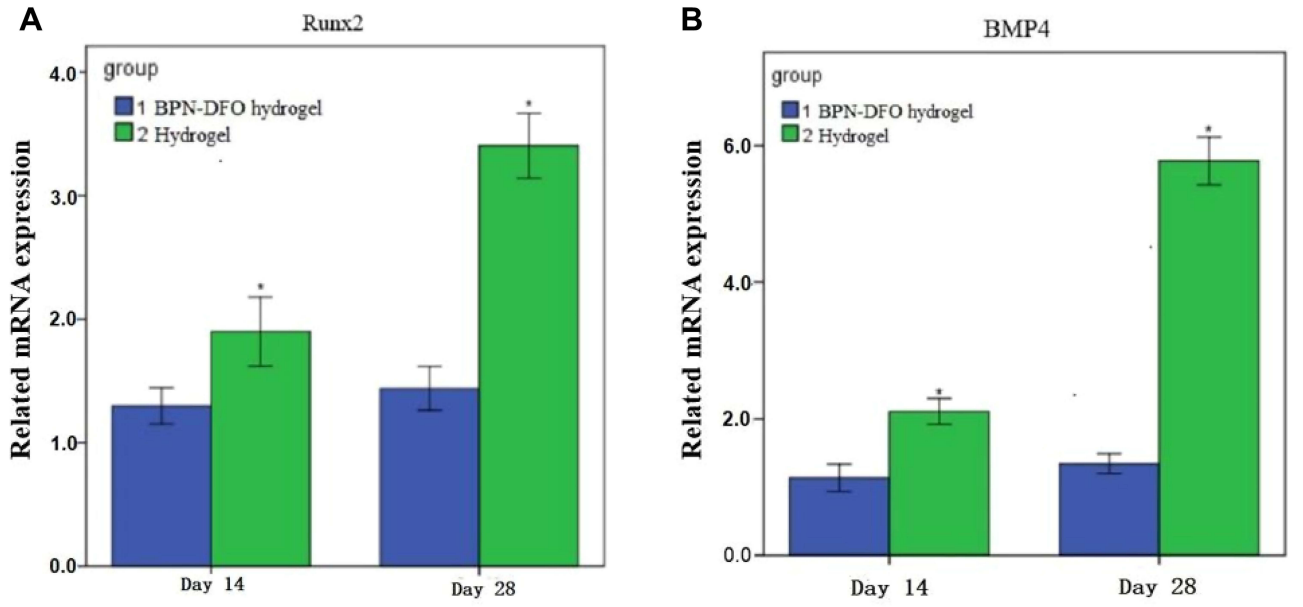

Figure 9 Summarized data showing the effect of BPN-DFO hydrogel and hydrogel on mRNA expression of BMP4 and Runx2 after culturing for 14 and 28 days in vivo. (**A**) The expression of Runx 2 in BPN-DFO group showed significantly improved than Hydrogel group at 14 and 28 days. (**B**) The expression of BPM 4 in BPN-DFO group showed significantly improved than Hydrogel group at 14 and 28 days. (*, $p<0.05$).

After the preparation of BPN-DFO hydrogel, such characteristics as its micro-structure, swelling, degradation and drug release were analyzed. Under the scanning electron microscope (SEM), After the observation of the surface of the BPN-DFO hydrogel, a microporous sponge-like structure was seen, which may be beneficial to cell growth and water absorption. As reported by Li et al, microporous structures can help cell and tissue grow by supplying more oxygen, nutrients and encapsulating cells.[43]

After that, the swelling rate and degradation rate was tested and compared. As showed in Figure 2A and B, better results are achieved for the BPN-DFO hydrogel in terms of swelling rate and degradation rate. The BPN-DFO hydrogel shows a faster degradation rate than the hydrogel, and the possible cause is that BPN can improve the hydrophilicity of the components.[44]

Then, release concentrations of phosphorus and ferric ion were also analyzed. As showed in Figure 3, BPN-DFO hydrogel can achieve sustained release of phosphorus ion. And a profile of initial burst release of ferric ion at first 24h with gradual increase after 48h was observed. The sustained release of phosphorus ion can have a positive effect on osteogenesis by synergizing with magnesium and calcium ions.[28] Besides, quickly released ferric ion can help vascularization during early stage,[45] preventing apoptosis and osteonecrosis by providing oxygen and nutrition for cell proliferation and tissue formation.

Biocompatibility of BPN-DFO hydrogel is the pivotal characteristic for the success of scaffold during bone regeneration. And as the outcome showed that adequate proliferation of live cells (Green) was found on days 1 and 3, meaning that BPN-DFO hydrogel have no cytotoxicity impact on hBMSC, which indicates BPN-DFO hydrogel have great potential to become a biocompatible scaffold.

In vitro osteogenic capability of hBMSC on BPN-DFO hydrogel was also evaluated and the RT-PCR test conducted for its quantitative determination. The bone regeneration related mRNA including Col I, BPM4 and Runx2, which are widely consider to be important marker for osteogenesis. The expression of Col I, BMP4 and Runx2 in BPN-DFO hydrogel was significantly higher than that in other two groups on days 7 and 14. Similarly, Li et al reported that the scaffold containing black phosphorus-based nanoparticles can achieve a significantly higher expression of osteogenesis relative mRNA than normal hydrogel scaffolds.[40] According to the previously reported results by Bestami et al, the cause may be that the BPN-DFO hydrogel can provide extra P^{5+}, thus promoting

osteogenesis by BMP−RUNX2 pathway.[46] Wu et al also reported that Black phosphorus nanosheets facilitates osteogenesis in the subsequent stage of bone healing.[47] Those results indicates that BPN-DFO hydrogel can promote the osteogenesis of hBMSC in Vitro.

Generally, these experimental results in Vitro verified that BPN-DFO hydrogel has an exciting effect on properties of hydrogel and osteogenesis of hBMSC. Also, the BPN-DFO hydrogel was implanted in Vivo for verifying the bone regeneration.

Besides, the samples were macroscopically evaluated and compared (6.24±0.68 VS 2.49±0.51; 9.36±0.48 VS 5.82 ±0.69. $P<0.05$), which primarily illustrates that BPN-DFO can yield superior bone regeneration and vascularization in bone defects.

Histological images including H&E, Masson staining and immunohistochemistry analysis were subsequently performed. H&E and Masson staining indicated that there was no inflammatory response or necrosis in the newly formed fibrous tissue of all groups. However, dense and mature newly-formed fibrous tissue and neovascularization were observed in BPN-DFO group, suggesting blood supply can promote the formation of fibrous tissue.[26] On the contrary, there was some loose newly-formed fibrous tissue and undegraded hydrogel without neovascularization existed in the hydrogel group. Some researchers reported that dense and mature newly-formed fibrous tissue and new blood vessel in H&E staining and Masson staining indicated better bone regeneration and angiogenesis.[48,49]

These phenomena suggest that bone regeneration at the ischemic bone defect site benefits from early neovascularization and mature fibrous tissue formation.

Kusumbe et al reported that CD31 strongly reflect the neovascularization during bone regeneration especially in the early stage, and deferoxamine (DFO) can enhance the CD31 expression by acting endothelial cells.[50] Stiller et al reported that collagen type I (COL I) was a pivotal part of osteogenesis.[51] As a consequence, the immunohistochemical test of CD31 and Col I for sections of ischemic tibial bone defects at weeks 2 and 4 was conducted (Figure 8). Much more immunofluorescence of Col I was shown in the new bone area in BPN-DFO hydrogel group, and CD31 was mainly localized in the cross area between new bone and normal bone, indicating that quickly released DFO can promote initial neovascularization and BPN can improve the expression of Col I, which is conductive to osteogenesis.

Yang et al and Kim et al reported that BMP4 could up-regulate of Runx2, which promoted osteogenesis of bone marrow mesenchymal stromal cells.[52,53] In order to verify whether BMP/Runx2 pathway is activated after BPN-DFO hydrogel implantation, the RT-PCR test of tibial sample grinding fluid including BMP4 and Runx2 were conducted (Figure 9). The expression of BMP4 and Runx2 increased significantly in BPN-DFO hydrogel group at weeks 2 and 4.

BPN is a new developed nano-material with superior biomedical applications, which can be degraded into phosphorus ions under the environment containing oxygen and water. Therefore, the phosphorus ion can be sustainably released when encapsulated into the hydrogel.[54] Phosphorus ion has a synergistic effect with calcium and can promote osteogenesis. The results of this study shows that BPN-DFO hydrogel can promote osteogenesis of ischemic tibial bone defects via BMP/Runx2 pathway. And Huang et al reported in a similar study that BPN-containing hydrogels improved osteogenic differentiation in vitro via BMP/Runx2 pathway.[30] Lu et al also reported that the lack of blood supply significantly impaired bone healing because adipogenic and fibrogenic proliferation and differentiation suppressed osteogenesis.[55] Neovascularization in the early stage plays a critical role in bone regeneration, which can effectively prevent bone nonunion. The possible reasons why BPN-DFO hydrogel promotes neovascularization at ischemic bone defect site are as follows: ferric ions from DFO can inhibit prolyl-hydroxylase proteins (PHD) and then simulate hypoxia, so that HIF1-α will not be rapidly degraded by PHD proteins.[56] Then HIF1-α can activate multiple hypoxia response genes involved in angiogenesis and regeneration.[26,57]

Limitation

This study has some limitations. A small sample of animals may limit the confidence level of this study, however significant difference was observed in the main results. Besides, although the Western blotting assay was not carried out due to the lack of samples, these results can primarily verify that BPN-DFO hydrogel can prevent nonunion of ischemic long bone defects by promoting osteogenesis and angiogenesis. A large number of animals still be needed for further study.

Conclusion

In the study, it is demonstrated that the BPN-DFO hydrogel has satisfactory swelling property, degradation rate and biocompatibility and it can promote proliferation and osteogenesis of hBMSC in vitro. Besides, the BPN-DFO hydrogel shows significant improvement in bone regeneration and neovascularization, which benefits cell proliferation and osteogenesis by providing oxygen and nutrition for cells in ischemic tibial bone defects of rats. What's more, quickly degraded hydrogel scaffolds not only possess osteoconductive but also provide more space for cells. Although more research is needed in the future, the biocompatibility and effectiveness of BPN-DFO hydrogel used in the clinical trials are still attracting great interest. Finally, the BPN-DFO hydrogel shows satisfactory results in rat models of acute ischemic tibial bone defects, which may become a useful material for some challenging situations, such as bone defects with artery injury, reoperation for nonunion and bone reconstruction.

Data Sharing Statement

The data that support this study are available within the article and available from the corresponding authors upon request.

Acknowledgment

This work was supported in part by grants from The Natural Science Foundation of Zhejiang, China (Grant No. LQ21H060002 and LGF20H060008), the National Natural Science Foundation of China (51803227), Social Welfare Research Key Project of Ningbo (2021S105), the S&T Innovation 2025 Major Special Program of Ningbo (2019B10063), and the Natural Science Foundation of Ningbo (Grant No.2019A610247).

Disclosure

The authors report no conflicts of interest in this work.

References

1. Jupiter JB, Leffert RD. Non-union of the clavicle. Associated complications and surgical management. *J Bone Joint Surg Am*. 1987;69(5):753–760. doi:10.2106/00004623-198769050-00018
2. ElHawary H, Baradaran A, Abi-Rafeh J, Vorstenbosch J, Xu L, Efanov JI. Bone Healing and Inflammation: principles of Fracture and Repair. *Semin Plast Surg*. 2021;35(3):198–203.
3. Herbert TJ, Fisher WE. Management of the fractured scaphoid using a new bone screw. *J Bone Joint Surg Br*. 1984;66(1):114–123.
4. Fani N, Farokhi M, Azami M, et al. Endothelial and Osteoblast Differentiation of Adipose-Derived Mesenchymal Stem Cells Using a Cobalt-Doped CaP/Silk Fibroin Scaffold. *ACS Biomater Sci Eng*. 2019;5(5):2134–2146.
5. Brinker MR, Hanus BD, Sen M, O'Connor DP. The devastating effects of tibial nonunion on health-related quality of life. *J Bone Joint Surg Am*. 2013;95(24):2170–2176.
6. Patil S, Montgomery R. Management of complex tibial and femoral nonunion using the Ilizarov technique, and its cost implications. *J Bone Joint Surg Br*. 2006;88(7):928–932.
7. Wen Y, Liu P, Wang Z, Li N. Clinical efficacy of bone transport technology in Chinese older patients with infectious bone nonunion after open tibial fracture. *BMC Geriatr*. 2021;21(1):488.
8. Piacentini F, Ceglia MJ, Bettini L, Bianco S, Buzzi R, Campanacci DA. Induced membrane technique using enriched bone grafts for treatment of posttraumatic segmental long bone defects. *J Orthop Traumatol*. 2019;20(1):13.
9. Feng D, Wang X, Sun L, et al. Double plating with autogenous bone grafting as a salvage procedure for recalcitrant humeral shaft nonunion. *BMC Musculoskelet Disord*. 2020;21(1):769.
10. Wiss DA, Garlich JM. Healing the Index Humeral Shaft Nonunion: risk Factors for Development of a Recalcitrant Nonunion in 125 Patients. *J Bone Joint Surg Am*. 2020;102(5):375–380.
11. Han X, Chang S, Zhang M, Bian X, Li C, Li D. Advances of Hydrogel-Based Bioprinting for Cartilage Tissue Engineering. *Front Bioengineering Biotechnol*. 2021;9:746564.
12. Xue W, Shi W, Kong Y, Kuss M, Duan B. Anisotropic scaffolds for peripheral nerve and spinal cord regeneration. *Bioactive Materials*. 2021;6(11):4141–4160.
13. Anderegg U, Halfter N, Schnabelrauch M, Hintze V. Collagen/glycosaminoglycan-based matrices for controlling skin cell responses. *Biol Chem*. 2021;402(11):1325–1335.
14. Shah SA, Sohail M, Khan SA, Kousar M. Improved drug delivery and accelerated diabetic wound healing by chondroitin sulfate grafted alginate-based thermoreversible hydrogels. *Mater Sci Eng C Mater Biol Appl*. 2021;126:112169.
15. Han X, He J, Wang Z, et al. Fabrication of silver nanoparticles/gelatin hydrogel system for bone regeneration and fracture treatment. *Drug Deliv*. 2021;28(1):319–324.
16. Kamel R, El-Wakil NA, Elkasabgy NA. Calcium-Enriched Nanofibrillated Cellulose/Poloxamer in-situ Forming Hydrogel Scaffolds as a Controlled Delivery System of Raloxifene HCl for Bone Engineering. *Int J Nanomedicine*. 2021;16:6807–6824.

17. Higgins JP, Borumandi F, Bürger HK, et al. Nonvascularized Cartilage Grafts Versus Vascularized Cartilage Flaps: comparison of Cartilage Quality 6 Months After Transfer. *J Hand Surg Am*. 2018;43(2):188.e181–188.e188.
18. Donneys A, Yang Q, Forrest ML, et al. Implantable hyaluronic acid-deferoxamine conjugate prevents nonunions through stimulation of neovascularization. *NPJ Regenerative Med*. 2019;4:11.
19. Li L, Li H, He Y, et al. Cyclic pulsation stress promotes bone formation of tissue engineered laminae through the F-actin/YAP-1/β-Catenin signaling axis. *NPJ Regenerative Med*. 2021;6(1):51.
20. Wang C, Ye X, Zhao Y, et al. Cryogenic 3D printing of porous scaffolds for in situ delivery of 2D black phosphorus nanosheets, doxorubicin hydrochloride and osteogenic peptide for treating tumor resection-induced bone defects. *Biofabrication*. 2020;12(3):035004.
21. Wang Z, Zhao J, Tang W, et al. Multifunctional Nanoengineered Hydrogels Consisting of Black Phosphorus Nanosheets Upregulate Bone Formation. *Small*. 2019;15(41):e1901560.
22. Wang X, Shao J, Abd El Raouf M, et al. Near-infrared light-triggered drug delivery system based on black phosphorus for in vivo bone regeneration. *Biomaterials*. 2018;179:164–174.
23. Lavin CV, Abbas DB, Fahy EJ, et al. A comparative analysis of deferoxamine treatment modalities for dermal radiation-induced fibrosis. *J Cell Mol Med*. 2021;1:847.
24. Geng M, Zhang Q, Gu J, et al. Construction of a nanofiber network within 3D printed scaffolds for vascularized bone regeneration. *Biomater Sci*. 2021;9(7):2631–2646.
25. Miao Y, Shi X, Li Q, et al. Engineering natural matrices with black phosphorus nanosheets to generate multi-functional therapeutic nanocomposite hydrogels. *Biomater Sci*. 2019;7(10):4046–4059.
26. Yan Y, Chen H, Zhang H, et al. Vascularized 3D printed scaffolds for promoting bone regeneration. *Biomaterials*. 2019;190:97–110.
27. Kiyama R, Nonoyama T, Wada S, et al. Micro patterning of hydroxyapatite by soft lithography on hydrogels for selective osteoconduction. *Acta Biomaterialia*. 2018;81:60–69.
28. Liu C, Yang G, Zhou M, et al. Magnesium Ammonium Phosphate Composite Cell-Laden Hydrogel Promotes Osteogenesis and Angiogenesis In Vitro. *ACS Omega*. 2021;6(14):9449–9459.
29. Aghayan HR, Hosseini MS, Gholami M, et al. Mesenchymal stem cells' seeded amniotic membrane as a tissue-engineered dressing for wound healing. *Drug Deliv Transl Res*. 2021.
30. Huang K, Wu J, Gu Z. Black Phosphorus Hydrogel Scaffolds Enhance Bone Regeneration via a Sustained Supply of Calcium-Free Phosphorus. *ACS Appl Mater Interfaces*. 2019;11(3):2908–2916.
31. Saleem MZ, Nisar MA, Alshwmi M, et al. Brevilin A Inhibits STAT3 Signaling and Induces ROS-Dependent Apoptosis, Mitochondrial Stress and Endoplasmic Reticulum Stress in MCF-7 Breast Cancer Cells. *Onco Targets Ther*. 2020;13:435–450.
32. Chai M, Gu C, Shen Q, et al. Hypoxia alleviates dexamethasone-induced inhibition of angiogenesis in cocultures of HUVECs and rBMSCs via HIF-1α. *Stem Cell Res Ther*. 2020;11(1):343.
33. Yang Y, Tang G, Yan J, et al. Cellular and molecular mechanism regulating blood flow recovery in acute versus gradual femoral artery occlusion are distinct in the mouse. *J Vasc Surg*. 2008;48(6):1546–1558.
34. Wayne JS, McDowell CL, Shields KJ, Tuan RS. In vivo response of polylactic acid-alginate scaffolds and bone marrow-derived cells for cartilage tissue engineering. *Tissue Eng*. 2005;11(5–6):953–963.
35. Wu M, Wu P, Xiao L, et al. Biomimetic mineralization of novel hydroxyethyl cellulose/soy protein isolate scaffolds promote bone regeneration in vitro and in vivo. *Int J Biol Macromol*. 2020;162:1627–1641.
36. Fávaro-Pípi E, Bossini P, de Oliveira P, et al. Low-intensity pulsed ultrasound produced an increase of osteogenic genes expression during the process of bone healing in rats. *Ultrasound Med Biol*. 2010;36(12):2057–2064.
37. Popescu I, Turtoi M, Suflet DM, et al. Alginate/poloxamer hydrogel obtained by thiol-acrylate photopolymerization for the alleviation of the inflammatory response of human keratinocytes. *Int J Biol Macromol*. 2021;180:418–431.
38. Chen H, Jia P, Kang H, et al. Upregulating Hif-1α by Hydrogel Nanofibrous Scaffolds for Rapidly Recruiting Angiogenesis Relative Cells in Diabetic Wound. *Adv Healthcare Mater*. 2016;5(8):907–918.
39. Demirtaş TT, Irmak G, Gümüşderelioğlu M. A bioprintable form of chitosan hydrogel for bone tissue engineering. *Biofabrication*. 2017;9(3):035003.
40. Li Z, Zhang X, Ouyang J, et al. Ca(2+)-supplying black phosphorus-based scaffolds fabricated with microfluidic technology for osteogenesis. *Bioactive Materials*. 2021;6(11):4053–4064.
41. Schierano G, Canuto RA, Mauthe von Degerfeld M, et al. Role of rhBMP-7, Fibronectin, And Type I Collagen in Dental Implant Osseointegration Process: an Initial Pilot Study on Minipig Animals. *Materials*. 2021;14:9.
42. Fernández-Martín S, Permuy M, López-Peña M, Muñoz F, González-Cantalapiedra A. No Effect of Long-Term Risedronate Use on Cartilage and Subchondral Bone in an Experimental Rabbit Model of Osteoarthritis. *Front Veterinary Sci*. 2020;7:576212.
43. Li Q, Xu S, Feng Q, et al. 3D printed silk-gelatin hydrogel scaffold with different porous structure and cell seeding strategy for cartilage regeneration. *Bioactive materials*. 2021;6(10):3396–3410.
44. Liu C, Pan L, Liu C, et al. Enhancing Tissue Adhesion and Osteoblastic Differentiation of MC3T3-E1 Cells on Poly(aryl ether ketone) by Chemically Anchored Hydroxyapatite Nanocomposite Hydrogel Coating. *Macromol Biosci*. 2021;21(7):e2100078.
45. Yang L, Ullah I, Yu K, et al. Bioactive Sr(2+)/Fe(3+)co-substituted hydroxyapatite in cryogenically 3D printed porous scaffolds for bone tissue engineering. *Biofabrication*. 2021;13(3):84.
46. Bastami F, Paknejad Z, Jafari M, Salehi M, Rezai Rad M, Khojasteh A. Fabrication of a three-dimensional β-tricalcium-phosphate/gelatin containing chitosan-based nanoparticles for sustained release of bone morphogenetic protein-2: implication for bone tissue engineering. *Mater Sci Eng C Mater Biol Appl*. 2017;72:481–491.
47. Wu Y, Liao Q, Wu L, et al. ZnL(2)-BPs Integrated Bone Scaffold under Sequential Photothermal Mediation: a Win-Win Strategy Delivering Antibacterial Therapy and Fostering Osteogenesis Thereafter. *ACS Nano*. 2021.
48. Sun T, Meng C, Ding Q, et al. In situ bone regeneration with sequential delivery of aptamer and BMP2 from an ECM-based scaffold fabricated by cryogenic free-form extrusion. *Bioactive Materials*. 2021;6(11):4163–4175.
49. Ren Z, Wang Y, Ma S, et al. Effective Bone Regeneration Using Thermosensitive Poly(N-Isopropylacrylamide) Grafted Gelatin as Injectable Carrier for Bone Mesenchymal Stem Cells. *ACS Appl Mater Interfaces*. 2015;7(34):19006–19015.

50. Kusumbe AP, Ramasamy SK, Itkin T, et al. Age-dependent modulation of vascular niches for haematopoietic stem cells. *Nature*. 2016;532 (7599):380–384.
51. Stiller M, Kluk E, Bohner M, Lopez-Heredia MA, Müller-Mai C, Knabe C. Performance of β-tricalcium phosphate granules and putty, bone grafting materials after bilateral sinus floor augmentation in humans. *Biomaterials*. 2014;35(10):3154–3163.
52. Yang J, McNamara LE, Gadegaard N, et al. Nanotopographical induction of osteogenesis through adhesion, bone morphogenic protein cosignaling, and regulation of microRNAs. *ACS Nano*. 2014;8(10):9941–9953.
53. Kim ME, Seon JK, Kang JY, Yoon TR, Lee JS, Kim HK. Bone-Forming Peptide-4 Induces Osteogenic Differentiation and VEGF Expression on Multipotent Bone Marrow Stromal Cells. *Front Bioengineering Biotechnol*. 2021;9:734483.
54. Hu Z, Li Q, Lei B, et al. Water-Catalyzed Oxidation of Few-Layer Black Phosphorous in a Dark Environment. *Angewandte Chemie*. 2017;56 (31):9131–9135.
55. Lu C, Miclau T, Hu D, Marcucio RS. Ischemia leads to delayed union during fracture healing: a mouse model. *J Orthopaedic Res*. 2007;25 (1):51–61.
56. Kusumbe AP, Ramasamy SK, Adams RH. Coupling of angiogenesis and osteogenesis by a specific vessel subtype in bone. *Nature*. 2014;507 (7492):323–328.
57. Jia P, Chen H, Kang H, et al. Deferoxamine released from poly(lactic-co-glycolic acid) promotes healing of osteoporotic bone defect via enhanced angiogenesis and osteogenesis. *J Biomed Mater Res A*. 2016;104(10):2515–2527.